DEVELOPMENT OF ATMOSPHERIC CHARACTERISTICS
OF CHLORINE-FREE ALTERNATIVE FLUOROCARBONS

REPORT ON R-134a & E-143a

Vladimir L. Orkin
Victor G. Khamaganov
Andrey G. Guschin
Eleanora E. Kasimovskaya
Igor K. Larin

Published April 1993

Report prepared by

for

CONTENTS

ABSTRACT

Rate constants have been measured for the gas phase reaction of OH radicals with 1,1,1,2-tetrafluoroethane R-134a (CH_2F-CF_3) and methyl trifluoromethyl ether E-143a (CH_3-O-CF_3) over the temperature range 298-460 K. The following Arrhenius expressions were derived to use for the atmospheric modeling:

$$k_{R-134a}(T) = (1.03 \, {}^{+0.10}_{-0.09}) \cdot 10^{-12} \cdot \exp\{-(1593 \pm 29)/T\} \, , \quad cm^3 molecule^{-1}s^{-1}.$$

$$k_{E-143a}(T) = (1.13 \pm 0.08) \cdot 10^{-12} \cdot \exp\{-(1330 \pm 23)/T\} \, , \quad cm^3 molecule^{-1}s^{-1}.$$

The infrared absorption cross-sections for R-134a and E-143a have been measured in the region from 400 to 1600 cm^{-1} and the integrated band strengths have been calculated.

The atmospheric lifetimes for R-134a and E-143a have been estimated to be 11.6 years and 4.1 years respectively. Global warming potentials have been estimated over time horizons of 20, 50, 100, 200, and 500 years:

Global warming potentials of R-134a and E-143a

	Time horizon (years)				
	20	50	100	200	500
R-134a	2420	1350	810	490	280
E-143a	1300	620	360	220	130

1. STUDY OF THE REACTIONS OF R-134a AND E-143a WITH OH

The presence of $\cdot$H atoms in R-134a and E-143a makes them reactive towards hydroxyl radicals ($\cdot$OH) in the troposphere. Moreover, these removal processes probably dictate atmospheric lifetimes of the substances (refs. 1-3). Therefore, the reliable and precise measurement of the rate constants for the reactions

$$\cdot OH + CH_3\text{-}O\text{-}CF_3 \xrightarrow{\ k_{E\text{-}143a}\ } H_2O + \cdot CH_2\text{-}O\text{-}CF_3 \tag{1}$$

$$\cdot OH + CH_2F\text{-}CF_3 \xrightarrow{\ k_{R\text{-}134a}\ } H_2O + \cdot CHF\text{-}CF_3 \tag{2}$$
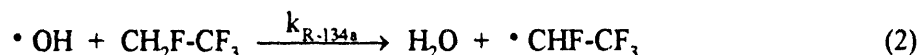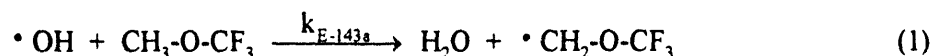
is the most relevant task in assessing the atmospheric lifetimes and possible role of R-134a and E-143a as "green-house" substances (ref. 1).

There is only one early study of reaction (1). The only rate constant reported (ref. 4) was at a temperature T= 296 K; that value was $k_{E\text{-}143a} = (2.14 \pm 0.15)\cdot 10^{-14}$ cm^{3}molecule^{-1}s^{-1}. References 5-10 report results of the rate constant measurements for reaction (2).

1.1 EXPERIMENTAL PROCEDURE

A discharge flow technique was used with electron paramagnetic resonance detection of the hydroxyl radicals. A scheme of the flow experiment is shown in Fig. 1. A 2.0 cm ID tubular reactor made of quartz was used. The inside surface of the reactor was covered with either F-32 or F-46 Teflon-like varnish to reduce wall loss of hydroxyl-radicals and prevent heterogeneous reactions. Linear flow velocities in the reactor of 700-1500 cm/s and total gas pressures of 0.8-3 Torr were used. The reactor was maintained with an accuracy of ± 0.3 K at the experimental temperature (in the range of 298-460 K) by passing either water or mineral oil through the outer jacket.

The gases were supplied to the flow reactor as admixtures in helium carrier gas (99.999% purity) that had been passed through liquid-nitrogen-cooled traps. Helium and the admixture of hydrogen (0.01-0.1%) were added to the reactor through a movable injector with a microwave discharge (2450 MHz, 10-20 W). The flows of helium with NO (~ 0.1%) and hydrohalocarbon under study were mixed upstream of the movable injector. The total pressure was measured at both ends of the reactor with an accuracy of ± 0.01 Torr. The flow rates of the carrier gas and reactants were determined directly by measuring the rate of pressure changes in calibrated volumes. The pressure measurements (the total pressure and the flow rates) are the major sources of instrumental error in the rate constant determinations. Absolute manometer calibrations to the water vapor pressure at the melting point [P_{H_2O} (T=273.15 K) = 4.58 Torr] were periodically used to prevent a systematic error. The overall instrumental error has been estimated to be less than 7% within a 95% confidence interval.

The hydroxyl radicals were generated in the fast reaction

$$\cdot H + NO_2 \rightarrow \cdot OH + NO \tag{3}$$

in the mixing zone near the injector. Thus, a movable source of $\cdot$OH radicals was used. The same reaction was used to determine the absolute concentration of $\cdot$OH by the chemical titration technique with monitoring of both $\cdot$OH radicals and $\cdot$H atoms. The concentration of $\cdot OH_{(v=0)}$ at the end of the reactor was measured using electron paramagnetic resonance

spectroscopy. Significant concentrations of vibrationally excited hydroxyl radicals (ref. 11) have not been detected in our experiments. Deactivation of $\bullet OH_{(v=1)}$ as a source of $\bullet OH_{(v=0)}$ could affect temporal profiles of hydroxyl concentration that might result in an error in rate constant measurement. The distance between the end of the injector and the center of the EPR-resonator (mode TE_{011}) was 4-30 cm. The absolute sensitivity for the $\bullet OH$ measurement was about $4 \cdot 10^9$ molecule/cm³ for a signal-to-noise ratio of unity with a 60-second integration time. Initial concentrations of $\bullet OH$ in the range 10^{11}-10^{12} molecule/cm³ were used.

The loss rate of $\bullet OH$ was obtained by measuring the $\bullet OH$ concentrations at various distances, z_0. Plots of $\ln\{[OH]\}$ versus z_0 were made to obtain the pseudo-first-order rate coefficients k':

$$k' = (k_W + k_{RH} \cdot [RH]) = v \cdot \frac{d \ln\{[OH]_0 / [OH]\}}{d z_0} , \qquad (4)$$

where k_W is the first order rate constant for the heterogeneous OH loss on the reactor wall, k_{RH} is the bimolecular rate constant for the reaction under study, and v is the average linear gas flow velocity. At each temperature, rate coefficients, k', were determined at various RH concentrations. The value of k_{RH} was then derived from a linear least-squares analysis of k' vs the concentration of hydrohalocarbon.

In such an experiment the length of the detection zone (length of EPR-resonator) does not cause an error in the rate constant being determined. This is true for the pseudo-first-order decay of the concentration of reactive particles along the reactor. In this case the concentration of $\bullet OH$ can be calculated (ref. 12) from the expression

$$[\bullet OH](z,\rho) \sim \exp\{-k'z/v\} \cdot \Phi\{\rho\} , \qquad (5)$$

where $\Phi\{\rho\}$ is the concentration distribution of active particles along the reactor radius ρ. The reactive particles flow along the reactor axis z to the detection zone; z_0 is the distance to the center of the EPR-resonator; R is the reactor radius; and L is the resonator length. Let the local sensitivity be determined by an arbitrary function $f(z-z_0, \rho)$, which is equal to zero outside the resonator, that is $f(z-z_0, \rho) = 0$ at $|z-z_0|>L/2$. In this case the signal (I) will be an integrated result over the resonator volume (when the injector is out of the resonator, i.e. $z_0 > L/2$):

$$I = \int_V [OH](z,\rho) \cdot f(z-z_0) \cdot dV = \int_{-\infty}^{\infty} \int_0^R 2\pi \cdot \rho \cdot \exp\{-k'z/v\} \cdot \Phi\{\rho\} \cdot f\{z-z_0, \rho\} \cdot d\rho \cdot dz \sim$$

$$\exp\{-k'z_0/v\} \cdot \int_{-L/2}^{L/2} \int_0^R \exp\{-k'(z-z_0)/v\} \cdot f\{(z-z_0), \rho\} \cdot \Phi\{\rho\} \cdot d\rho \cdot d(z-z_0) . \qquad (6)$$

The last integral in Eq. (6) does not depend on z_0; therefore, Eq. (4) gives the exact value of k' independent of L and $f(z,\rho)$.

1.2 SAMPLE PURITY

A main source of error in measurement of the reaction rate constant can be the presence of reactive impurities in the sample under study. The sample of E-143a used for this investigation was analyzed by gas chromatography. The stated purity was 99.44% for gas phase sampling

2

and 99.90% for liquid phase sampling. Therefore, the rate constant for the reaction under study could easily be overestimated if impurities react with $\cdot$ OH much faster than $CH_3\text{-}O\text{-}CF_3$. The sample of E-143a was purified by distillation to obtain the material used for the reaction rate measurement. Several other fractions with different levels of impurities also were obtained. The levels of impurities for fractions used in this study as measured by gas chromatography are listed in Table 1. 'E-1-g' and 'E-1-l' are the gas and liquid phase, respectively, of the original sample. 'E-2', 'E-3', and 'E-4' are the various fractions; 'E-4' is the purest one.

Table 1. Levels of impurities in E-143a samples used in this study (%), as determined by gas chromatography

Sample	Retention time (min)				
	1.21	1.40	1.78	1.92	2.80
E-1-g	0.16	0.36	0.03	0.01	99.44
E-1-l	0.027	0.083	-	-	99.89
E-2	0.084	0.158	0.031	0.027	99.70
E-3	0.016	-	-	-	99.984
E-4	0.006	-	-	-	99.994

The sample of R-134a was analyzed especially for the presence of unsaturated halocarbons. The purity of the sample was stated as $[CH_2F\text{-}CF_3]$ > 99.98%. The stated content of unsaturated halocarbons (ethenes, propenes) did not exceed 5 ppm.

1.3 RESULTS AND DISCUSSION

In order to obtain reliable results, we investigated the E-143a samples of different purity levels listed in Table 1. The control experiments were done at T = 298 K for all the samples. Rate constants for the reactions of $\cdot$ OH with more reactive impurities should have less temperature dependence; therefore, these impurities should have the most influence at the lowest temperature. The value of the rate constants obtained coincided within ~5% for all the samples with very different levels of measured impurities.

Secondary reactions of $\cdot$ OH with products of the reaction under study could be another source of error. If the $\cdot$ OH loss in such reactions were significant under the experimental conditions, overestimation of the bimolecular rate constant k_{RH} would result. Computer simulations show that the increase of the reaction rate constant (if there is any) has to depend on the initial hydroxyl concentration. However, in our experiments with both R-134a and E-143a, neither $k_{R\text{-}134a}$ nor $k_{E\text{-}143a}$ changed within experimental error; while the $\cdot$ OH initial concentrations varied from ~$1.5 \cdot 10^{11}$ molecule/cm^3 up to $6 \cdot 10^{11}$ molecule/cm^3. The experiments were carried out at both 298 K and 370 K.

Therefore, we are confident that the rate constants obtained characterize the reactions of $\cdot$ OH with $CH_2F\text{-}CF_3$ and $CH_3\text{-}O\text{-}CF_3$, respectively. The results of the rate constant measurements are listed in Table 2 and Table 3. The error values represent 95% confidence intervals and include estimated systematic errors. The results in Table 2 were obtained using the most pure E-143a sample.

Table 2. Kinetic data for the reaction of hydroxyl radicals with CH_3-O-CF_3 (E-143a)

Temperature (K)	[CH_3-O-CF_3] range (10^{15} molecule/cm^3)	Number of experiments	k_{E-143a} (10^{-14} cm^3molecule^{-1}s^{-1})
298	0.2 - 5.3	18	1.30 ± 0.09
308	0.4 -2.2	2	1.50 ± 0.20
319	0.4 - 2.4	3	1.76 ± 0.16
330	0.4 - 1.3	1	1.88 ± 0.25
342	0.5 -2.8	3	2.31 ± 0.16
355	0.2 - 2.2	2	2.73 ± 0.22
370	0.4 - 2.6	7	3.08 ± 0.21
410	0.2 - 1.5	2	4.56 ± 0.42
460	0.2 - 1.1	2	6.00 ± 0.48

Figure 2 shows the results of the measurements of k_{E-143a} together with those reported in ref. 4. The Arrhenius dependence for the rate constant derived from our data and the curves that restrict the 95% confidence intervals for the mean k_{143a} value are also shown in Fig. 2. The following Arrhenius expression was derived from our data obtained between 298 and 460 K:

$$k_{E-143a}(T) = (1.13 \pm 0.08) \cdot 10^{-12} \cdot \exp\{-(1330 \pm 23)/T\}, \quad cm^3molecule^{-1}s^{-1} \qquad (7)$$

Uncertainties in the pre-exponential and exponential term are expressed as 95% confidence intervals.

The value of k_{143a} measured in this work is essentially lower than the one reported in ref. 4. The reason for such a discrepancy is not clear. It likely is connected with the presence of unresolved reactive microimpurities in the sample used in ref. 4. There are no other reported data for this reaction.

Table 3. Kinetic data for the reaction of hydroxyl radicals with CH_2F-CF_3 (R-134a)

Temperature (K)	[CH_2F-CF_3] range (10^{15} molecule/cm^3)	Number of experiments	k_{R-134a} (10^{-14} cm^3molecule^{-1}s^{-1})
298	0.5 - 5.9	10	4.97 ± 0.42
313	0.6 -4.1	1	6.27 ± 0.44
330	0.7 - 4.8	4	8.12 ± 0.65
350	0.7 - 4.5	2	10.85 ± 0.76
360	0.5 -4.0	2	12.0 ± 1.10
370	0.5 - 3.5	5	14.3 ± 1.20
410	0.3 - 1.4	1	26.2 ± 2.7
460	0.3 - 2.2	7	41.1 ± 4.4

Figure 3 shows the results of the measurements of k_{R-134a} together with those reported in refs. 5-10. The Arrhenius dependence for the rate constant derived from our data and the curves that restrict the 95% confidence intervals for the mean k_{R-134a} value are also shown in Fig. 3. There is some positive curvature in the temperature dependence at high temperatures.

Keeping in mind the atmospheric implications of these results, the following Arrhenius expression was derived from our data obtained between 298 and 370 K:

$$k_{R-134a}(T) = (1.03 \, {}^{+0.10}_{-0.09}) \cdot 10^{-12} \cdot \exp\{-(1593 \pm 29)/T\} , \quad cm^3 molecule^{-1} s^{-1}. \qquad (8)$$

Uncertainties in the pre-exponential and exponential term are expressed as 95% confidence intervals.

Our value of k_{R-134a} is in excellent agreement with that reported in ref. 5. Within the errors reported (~8% at 95% confidence intervals), the results coincide over the whole temperature range. Moreover, the Arrhenius dependence derived in the present work describes the low-temperature data reported in ref. 5 quite well. At T = 298 K, the value of k_{R-134a} coincides with the results reported in ref. 6 and ref. 7. The difference between our data and those obtained in ref.6 is up to 40% at T= 400 K. Note that the data reported in ref. 5 and ref. 6 were apparently obtained for the same R-134a samples; therefore, the discrepancies between these data are due to the different techniques used. The rate constant reported in ref. 8 is 20% - 40% higher than our values above room temperature and ~50% higher than our extrapolated results and those reported in ref. 5 below room temperature. Possible reasons for such a discrepancy are the presence of reactive impurities in the samples as well as heterogeneous reactions that could occur in the reactor used in ref. 8. The second supposition is confirmed by the reported curvature of the pseudo-first order plots for at least their experiments below room temperature. The overestimation of the k_{R-134a} value obtained in ref. 9 and in ref. 10 using the flow technique may well be accounted for by the reasons given above.

2. SPECTRAL MEASUREMENTS

2.1 ULTRAVIOLET RANGE (190-340 nm)

Ultraviolet absorption cross-sections of both R-134a and E-143a were measured between 190 and 340 nm in the 14 cm quartz absorption cell at 750 Torr and 295 K with a 'Specord-M40' double beam spectrophotometer. Absorptions down to 0.0001 abs. units were measured.

Absorption of the R-134a sample was less than 0.001 abs. units over the whole range. Therefore, the absorption cross-sections of CH_2F-CF_3 in this range are less than ~10^{-23} cm^2/molecule, and the photolysis thus does not contribute to the atmospheric lifetime of R-134a.

Noticeable absorption of E-143a samples over the whole region have been measured, with two bands having resolved vibrational structures between 190 and 230 nm, as well as between 230 and 330 nm. The atmospheric lifetime calculation should be affected by the tropospheric photolysis if the absorption in the range 280-330 nm was due to CH_3-O-CF_3 molecules. The absorption cross-sections were small and changed with the sample purity. Slight absorption was still measured even with the purest sample, 'E-4'. So this absorption seems to be mainly due to the presence of impurities in the samples.

Another fluoroether, E-152a ($CH_3-O-CHF_2$) was studied to determine if such ethers have absorption in the 280-340 nm range. The absorption cross-sections of $CH_3-O-CHF_2$ (E-152a) do not exceed ~10^{-24} cm^2/molecule in this wavelength range. Such absorption does not contribute to the decrease of atmospheric lifetimes due to photolysis in the troposphere. This

confirms that the absorption measured in the 280 - 330 nm range of E-143a samples is due to the spectra of microimpurities.

2.2 INFRARED RANGE (400-1600 cm^{-1})

The infrared absorption cross sections were measured with a double-beam, diffraction 'Specord M-80' spectrophotometer at a temperature T = 295 K. The spectra were recorded with an increment of 0.2 cm^{-1} and with a spectral slit width of 0.5 cm^{-1}. The pressure inside the absorption cell was measured by a bellows inductive manometer with an accuracy of ±0.01 Torr. The results presented here were obtained by using a 12.16 ± 0.02 cm glass cell fitted with KBr windows. Absorption spectra of the evacuated and filled cell were recorded to determine absorption cross-sections using the Beer-Lambert law. The overall instrumental uncertainty connected with measurements of path length, pressure, temperature stability, and absorption was estimated to be less than 2%.

The base e absorbances obtained were converted to absorption cross-sections through the following relationship:

$$\sigma(\nu) = \frac{\ln\{I_0(\nu)/I(\nu)\}}{[RH]\cdot l} \qquad (9)$$

where

ν = the wavenumber, in units of cm^{-1};
$\sigma(\nu)$ = the absorption cross-section at wavenumber ν, in units of cm^2/molecule;
$I_0(\nu)$ = the intensity of the incident radiation at wavenumber ν;
$I(\nu)$ = the intensity of the transmitted radiation at wavenumber ν;
[RH] = the concentration of hydrohalocarbon under study, in units of molecules/cm^3;
l = the optical path length in centimeters.

The IR absorption cross-sections are shown in Fig. 4 and Fig. 5 for CH_3-O-CF_3 and CH_2F-CF_3, respectively. For the features of interest, integrated band strengths listed in Table 4 and Table 5 were calculated with the following expression:

$$\sigma_{IBS}(\nu_1 - \nu_2) = \int_{\nu_1}^{\nu_2} \sigma(\nu)\cdot d\nu. \qquad (10)$$

The limits of integration were chosen arbitrarily to give numerics for each feature only.

Table 4. Integrated band strengths of CH_3-O-CF_3 (E-143a)

Wavenumbers (cm^{-1})	Band strengths (10^{-17} cm^{2}molecule^{-1}cm^{-1})
410 - 480	0.078 ± 0.001
480 - 680	0.176 ± 0.003
800 - 890	0.119 ± 0.002
970 - 1105	0.564 ± 0.006
1105 - 1210	7.190 ± 0.093
1210 - 1405	12.20 ± 0.15
1405 - 1600	1.043 ± 0.006

6

To confirm the applicability of the data obtained for atmospheric modeling, the results were obtained:

i - There were no changes in the integrated absorption band strengths when the absorption cell containing the sample of either E-143a or R-134a was pressurized to 700 Torr with dry air or nitrogen.

ii - There were no changes in the integrated absorption band strengths when the spectral slit was varied in the range of 0.5-2.0 cm^{-1}.

iii - The absorption cross-sections were obtained at several pressures for each band to confirm the correctness of the Beer-Lambert law. There were no deviations from it when absorbance was less than ~1.0.

Integrated band strengths for the spectral regions were determined from plots of integrated area vs concentration of the substance under study. Figures 6 and 7 show the plots for all the bands of E-143a that were defined. Figure 8 shows the plots for the bands of R-134a. A least squares fit to the data points for each region was made to derive σ_{IBS} values, which are given with their 95% confidence intervals in Tables 4 and 5. Table 5 presents results on R-134a, as well as the data reported in ref. 13.

Table 5. Integrated band strengths of CH_2F-CF_3 (R-134a)

Wavenumbers (cm^{-1})	Band strengths (10^{-17} cm^{2}molecule^{-1}cm^{-1})		
	This work		ref. 18
490 - 600	0.148 ± 0.002		-
600 - 700	0.512 ± 0.005		0.555
800 - 920	0.272 ± 0.004		0.335
920 - 1030	0.916 ± 0.012		
1030 - 1140	1.492 ± 0.018	7.877	7.816
1140 - 1250	5.469 ± 0.033		
1250 - 1350	4.171 ± 0.021	4.269	4.229
1350 - 1395	0.098 ± 0.002		
1395 - 1448	0.330 ± 0.006		-
1448 - 1510	0.154 ± 0.003		-
1510 - 1550	0.018 ± 0.006		-
1510 - 1550	0.018 ± 0.006		-

3. ATMOSPHERIC IMPLICATIONS

The atmospheric lifetime of hydrogen containing substances such as E-143a and R-134a can be estimated in the following manner (ref. 2, 3):

$$\tau_{RH} = \tau_{MC} \cdot k_{MC}(277)/k_{RH}(277). \tag{11}$$

Here $k_{RH}(277)$ and $k_{MC}(277)$ are the rate constants for the reactions of OH with the hydrohalocarbon under consideration and with methyl chloroform, respectively, at T= 277 K. The value $k_{MC}=1.8\cdot10^{-12}\cdot\exp\{-1550/T\}$ cm³molecule⁻¹s⁻¹ for the reaction between • OH and methyl chloroform is now recommended (ref. 14). The recommendation is based on recent investigations of this reaction (ref. 15-17). The atmospheric lifetime of methyl chloroform ($\tau_{MC} = 5.7^{+0.7}_{-0.6}$ years) has been derived on the basis of field measurements of its atmospheric trends (ref. 18). According to ref. 17, T = 277 K is the optimum temperature for such scaling. The rate constant k_{E-143a} at T = 277 K is estimated to be $9.3\cdot10^{-15}$ cm³molecule⁻¹s⁻¹, based on our data. Based on this data, the atmospheric lifetime of E-143a is estimated to be 4.1 years. Note that the atmospheric lifetime of E-143a is approximately 15 times less than that of the analogous alkane R-143a (ref. 1).

Reference 4 reports the atmospheric lifetime of E-143a to be 3.0 years. This discrepancy is attributable to the difference in the rate constant values obtained. Moreover, the atmospheric lifetime was estimated in ref. 4 by using the 'scaling' at T = 296 K. This resulted in some overestimation of τ_{E-143a} due to the difference in the temperature dependencies of the rate constants k_{E-143a} and k_{MC}. Reference 19 reports the theoretically predicted atmospheric lifetime of E-143a to be 0.6 years. Comparison with the value obtained in this work confirms the need for experimental studies in assessing the environmental properties of substances.

The rate constant k_{R-134a} at T = 277 K is estimated to be $3.28\cdot10^{-15}$ cm³molecule⁻¹s⁻¹, based on our data; and $3.26\cdot10^{-15}$ cm³molecule⁻¹s⁻¹ and $2.81\cdot10^{-15}$ cm³molecule⁻¹s⁻¹, based on data reported in ref. 5 and ref. 6, respectively. Based on our data, the atmospheric lifetime of R-134a is estimated to be 11.6 years.

Direct halocarbon global warming potentials (hGWP) (ref. 18) have been calculated for different time horizons based on the estimated atmospheric lifetime and measured infrared absorption cross-sections of the hydrohalocarbon under study, taking into account the spectrum of Earth's outgoing infrared radiation. Table 6 represents the values obtained for R-134a. Based on the currently adopted values of direct GWP of CFC-11 over different time horizons (ref. 1), GWPs of R-134a have been estimated. Our estimations of GWPs using the atmospheric lifetime of 15.6 years adopted in ref. 1 (GWP-15.6) are presented in Table 6, as well as the GWPs reported in ref. 1 (GWP -ref. 1). Table 7 represents the values obtained for E-143a.

Table 6. Global warming potentials of R-134a

	Time horizon (years)				
	20	50	100	200	500
Halocarbon global warming potentials	0.54	0.33	0.24	0.205	0.20
Global warming potentials	2420	1350	810	490	280
Global warming potentials (τ_{R-134a} = 15.6)	2860	1770	1090	660	380
Global warming potentials (ref. 1)	3100	1900	1200	730	400

Table 7. Global warming potentials of E-143a

| | Time horizon (years) | | | | |
	20	50	100	200	500
Halocarbon global warming potentials	0.29	0.15	0.107	0.092	0.090
Global warming potentials	1300	620	360	220	130

4. REFERENCES

1. World Meteorological Organization Global Ozone Research and Monitoring Project, Report No.25, *Scientific Assessment of Ozone Depletion* (1991).

2. M. Prather and C. M. Spivakovsky, "Tropospheric OH and the Lifetimes of Hydrofluorocarbons," *J. Geophys. Res.* **95**, 18723-29 (1990).

3. V. L. Orkin and V. G. Khamaganov, "Determination of Rate Constants for Reactions of Some Hydrohaloalkanes with OH Radicals and their Atmospheric Lifetimes," *J. Atmos. Chem.* **16**, 157-67 (1993).

4. Z. Zhang, R. D. Saini, M. J. Kurylo and R. E. Huie, "Rate Constants for the Reactions of the Hydroxyl Radical with Several Partially Fluorinated Ethers," *J. Phys. Chem.* **96**, 9301-9304 (1992).

5. T. Gierczak, R. Talukdar, G. L. Vaghjiani, E. R. Lovejoy and A. R. Ravishankara, "Atmospheric Fate of Hydrofluoroethanes and Hydrofluorochloroethanes: 1. Rate Coefficients for Reactions with OH," *J. Geophys. Res.* **96**, 5001-5011 (1991).

6. R. Liu, R. E. Huie and M. J. Kurylo, "Rate Constants for the Reactions of OH Radical with Some Hydrochlorofluorocarbons over the Temperature Range 270-400 K," *J. Phys. Chem.* **94**, 3247-49 (1990).

7. J. P. Martin and G. Paraskevopoulos, "A Kinetics Study of the Reactions of OH Radicals with Fluoroethanes. Estimates of C-H Bond Strengths in Fluoroalkanes," *Can. J. Chem.* **61**, 861-65 (1983).

8. A. C. Brown, C. E. Canosa-Mas, A. D. Parr and R. P. Wayne, "Laboratory Studies of Some Halogenated Ethanes and Ethers: Measurements of Rates of Reaction with OH and of Infrared Absorption Cross-Sections," *Atmospheric Environment* **24A**, 2499-2511 (1990).

9. M. A. A. Clyne and P. M. Holt, "Reaction Kinetics Involving Ground $X^2\Pi$ and Excited $A^2\Sigma^+$ Ra..●Part 2. Rate Constant for Reactions of OH $X^2\Pi$ with Halogenomethanes and Halogenoethanes," *J. Chem. Soc. Faraday Trans. 2* **75**, 582-91 (1979).

10. K. M. Jeong, K. J. Hsu, J. B. Jeffries and F. Kaufman, "Kinetics of the Reactions of OH with C_2H_6, CH_3CCl_3, $CH_2ClCHCl_2$, $CH_2ClCClF_2$, and CH_2FCF_3," *J. Phys. Chem.* **88**, 1222-26 (1984).

11. J. E. Spencer and G. P. Glass, "The Reaction of Atomic Hydrogen with NO_2," *Chem. Phys.* **15**, 35-41 (1976).

12. R. L. Brown, "Tubular Flow Reactor with First-Order Kinetics," *J. Res. Natl. Bur. Stand. (U.S.)* **83**, 1-8 (1978).

13. D. A. Fisher, C. H. Hales, W. C. Wang, M. K. W. Ko and N. D. Sze, "Model Calculations of the Relative Effects of CFCs and their Replacements on Global Warming," *Nature* **344**, 513-16 (1990).

14. W. B. DeMore, S. P. Sander, D. M. Golden, M. J. Molina, R. F. Hampson, M. J. Kurylo, C. J. Hovard and A. R. Ravishankara, "Chemical Kinetics and Photochemical Data for Use in Stratospheric Modeling," Evaluation No. 10, *JPL Publication* **92-20** (1992).

15. R. K. Talukdar, A. Mellouki, A. M. Schmoltner, T. Watson, S. Montzka and A. R. Ravishankara, "Kinetics of the OH Reaction with Methyl Chloroform and its Atmospheric Implications," *Science* **257**, 227-30 (1992).

16. W. B. DeMore, "Relative Rate Constant for the Reactions of OH with Methane and Methyl Chlorophorm," *Geophys. Res. Lett.* **19**, 1367-70 (1992).

17. B. J. Finlayson-Pitts, M. J. Ezell, T. M. Jayaweera, H. N. Berko and C. C. Lai, "Kinetics of the Reactions of OH with Methyl Chlorophorm and Methane: Implications for Global Tropospheric OH and the Methane Budget," *Geophys. Res. Lett.* **19**, 1371-74 (1992).

18. R. Prinn, D. Cunnold, P. Simmonds, F. Alyea, R. Boldy, A. Crawford, P. Fraser, D. Gutzler, D. Hartley, R Rosen and R. Rasmussen, "Global Average Concentration and Trend for Hydroxyl Radicals Deduced from ALE/GAGE Trichloroethane (Methyl Chloroform) Data for 1978-1990," *J. Geophys. Res.* **97**, 2445-51 (1992).

19. D. L. Cooper, T. P. Cunningham, N. L. Allan and A. McCulloch, "Tropospheric Lifetimes of Potential CFC Replacements: Rate Coefficients for Reaction with the Hydroxyl Radical," *Atmospheric Environment* **26A**, 1331-34 (1992).
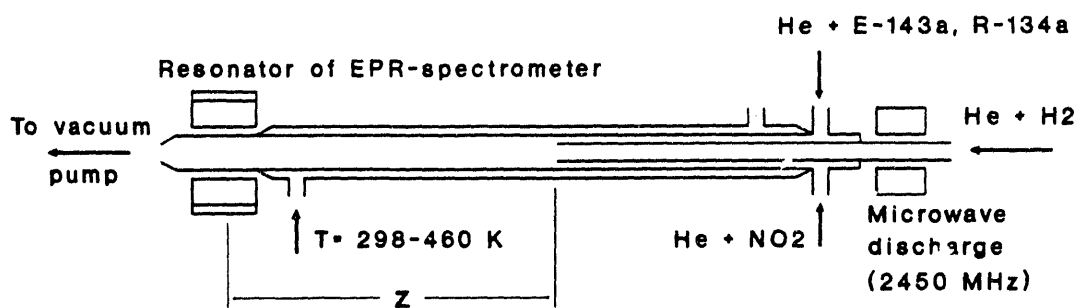
10

5. FIGURES

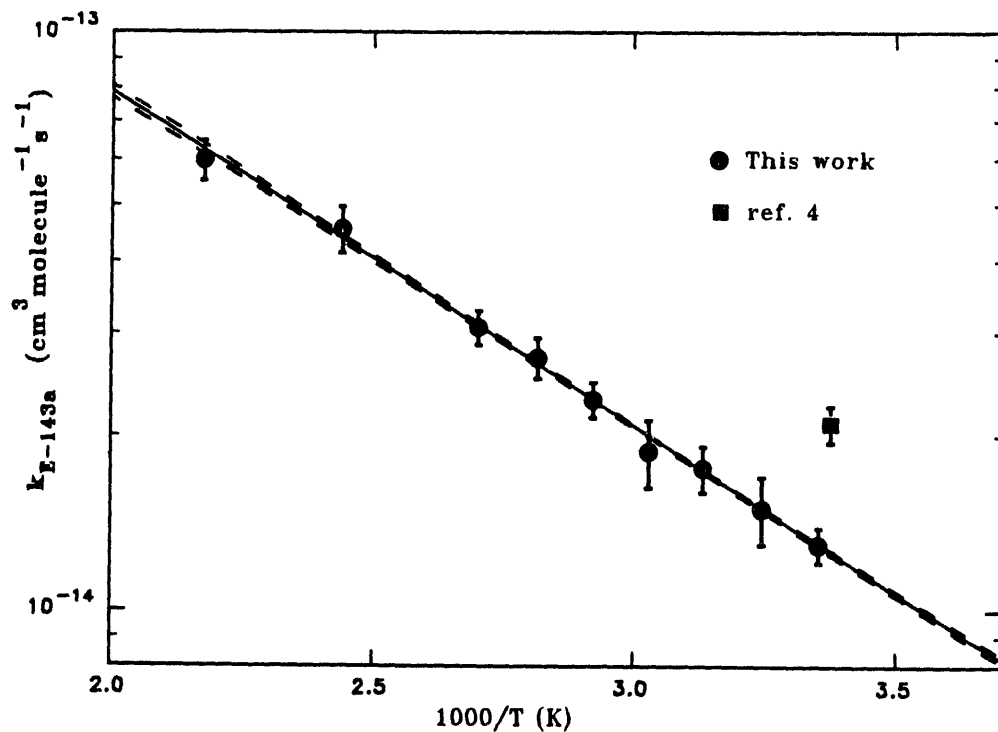Fig. 1. Scheme of the flow experiment.

Fig. 2. Plot of the measured k_{E-143a} values vs 1/T and the least-squares fit to our data (solid line) with its 95% confidence intervals (dashed lines).
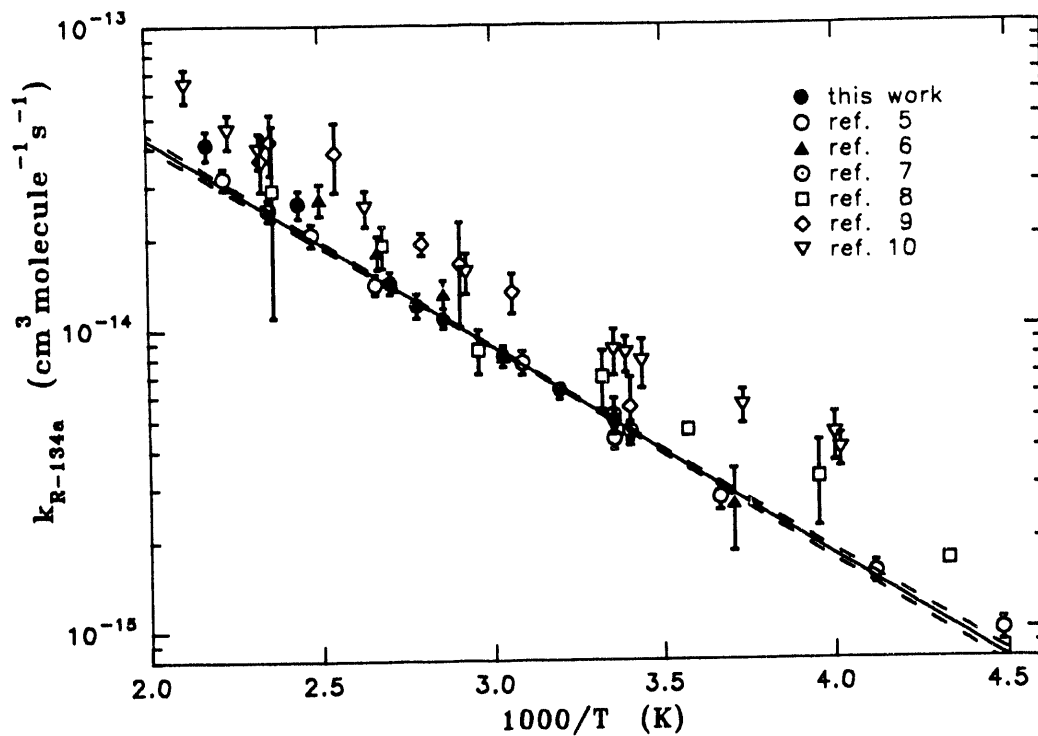
Fig. 3. Plot of the measured k_{R-134a} values vs 1/T and the least-squares fit to our data (solid line) with its 95% confidence intervals (dashed lines).
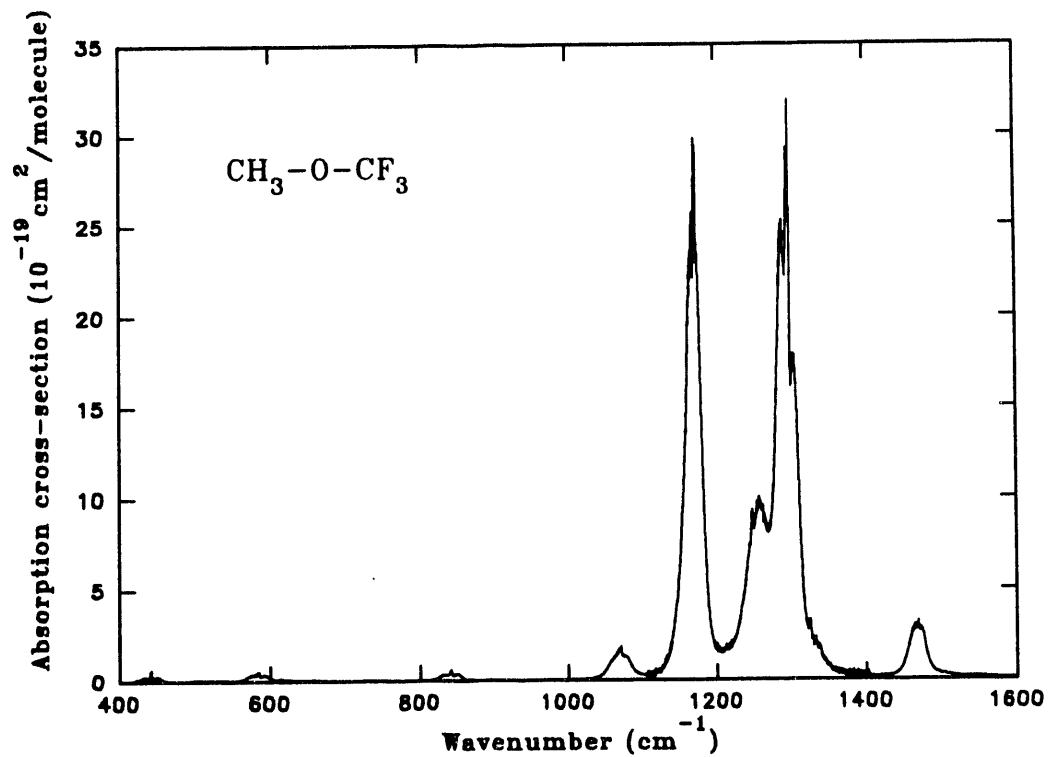

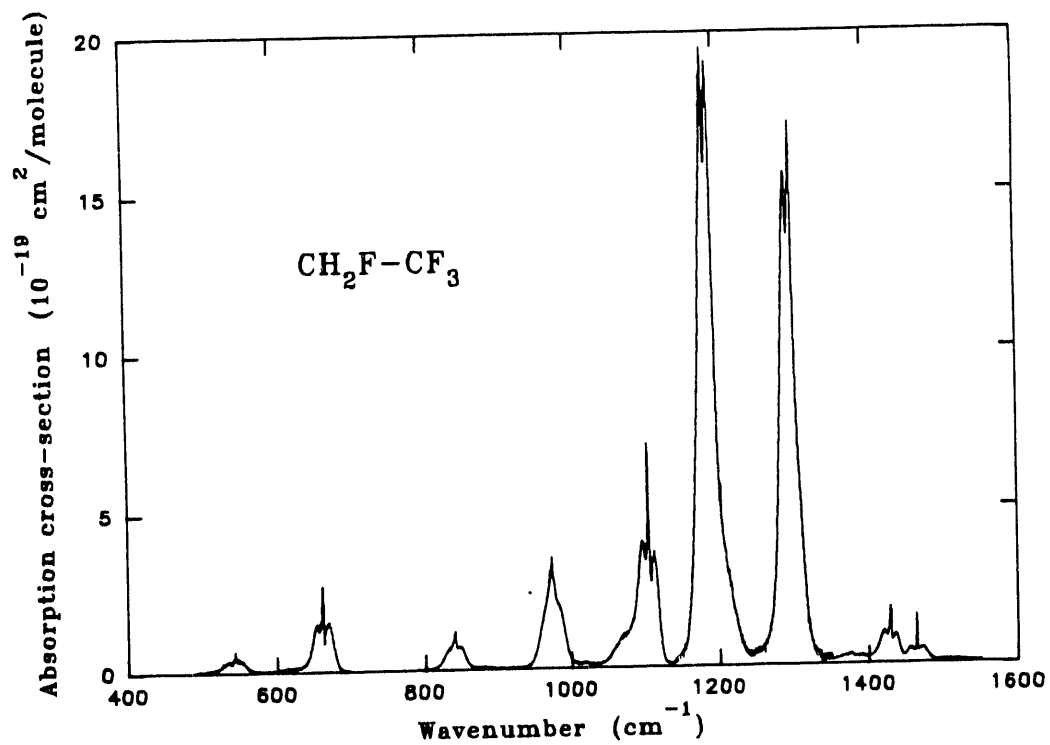**Fig. 4. Infrared absorption cross-sections of CH_3-O-CF_3 (E-143a) (resolution is 0.5 cm⁻¹).**

Fig. 5. Infrared absorption cross-sections of CH_2F-CF_3 (R-134a) (resolution is 0.5 cm^{-1}).
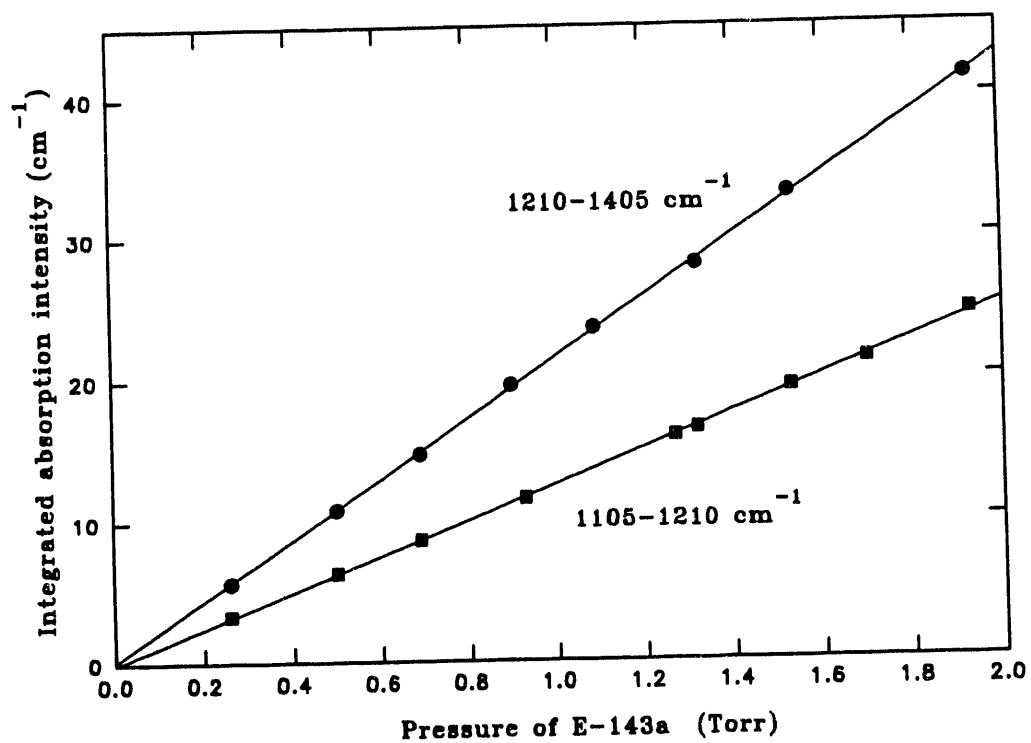

Fig. 6. Dependence of integrated intensity (base e) on E-143a pressure for strongest absorption bands.
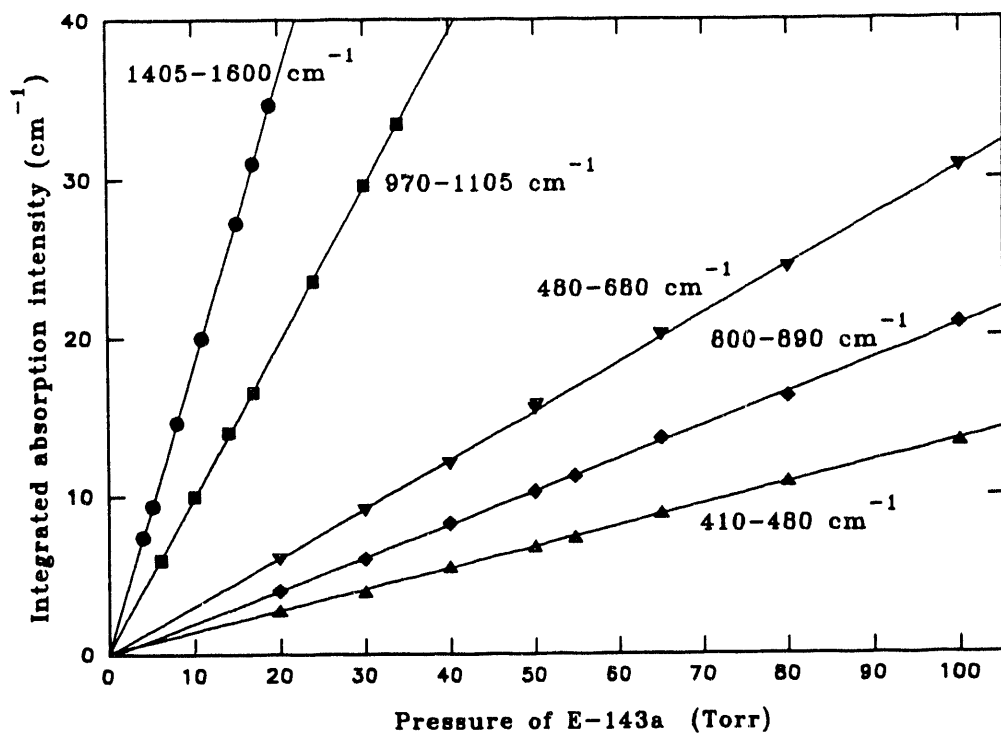
Fig. 7. Dependence of integrated intensity (base *e*) on E-143a pressure.
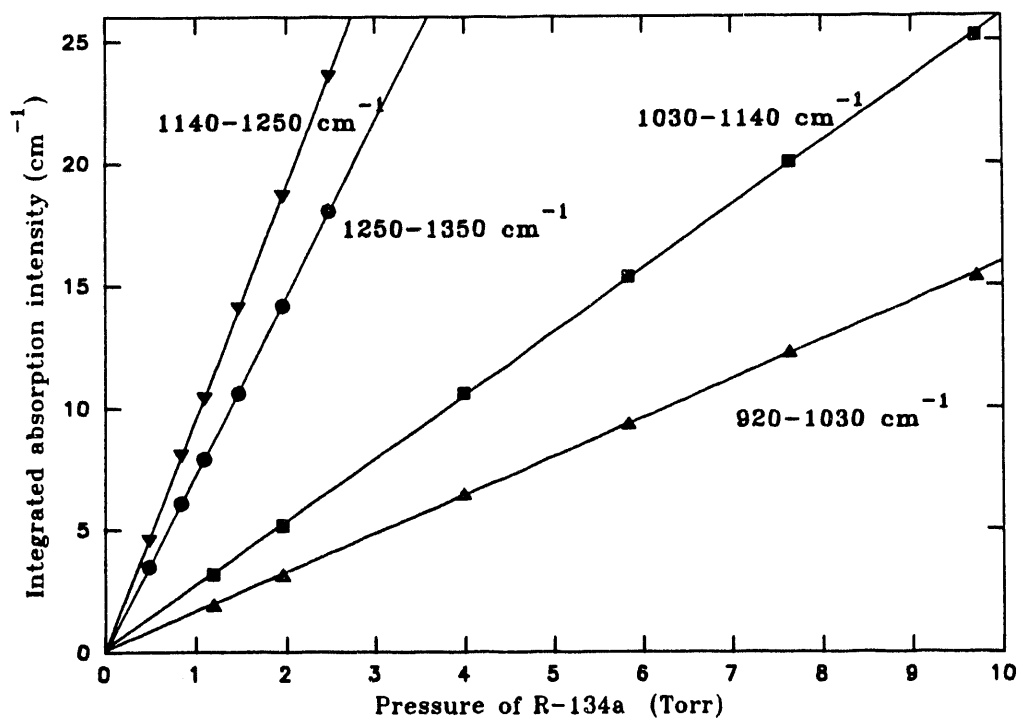

Fig. 8. Dependence of integrated intensity (base *e*) on R-134a pressure for strongest absorption bands.

INTERNAL DISTRIBUTION

1. K. R. Ballew
2. V. D. Baxter
3. D. M. Counce
4. G. E. Courville
5. N. Dominguez
6. P. D. Fairchild
7. W. Fulkerson
8. M. A. Kuliasha
9. C. I. Moser
10. J. R. Sand
11. R. B. Shelton
12. ORNL Patent Office1
13. Central Research Library
14. Document Reference Section
15-17. Lab Records
18. Lab Records - Record Copy

EXTERNAL DISTRIBUTION

19. J. L. Adcock, University of Tennessee, Knoxville, Tn 37996-1600.

20. A. L. Beyerlein, Department of Chemistry, Clemson University, Clemson, S. C. 29634-1905

21. D. B. Bivens, Ph.D., DuPont Chemicals, Fluorochemicals Laboratory, Chestnut Run Plaza, P.O. Box 80711, Wilmington, DE 19880-0711.

22. D. R. Bohi, Resources for the Future, 1616 P Street, NW, Washington, DC 20036

23. D. D. Des Marteau, Department of Chemistry, Clemson University, Clemson, S. C. 29634-1905

24. T. E. Drabek, University of Denver, Denver, CO 80208-0209.

25. D. Fischer, E 320/290, E. I. DuPont de Nemours Inc., Scientific Computing Division, Experimental Station, Rt. 141, Bldg. 320, P.O. Box 80320, Wilmington, DE 19880-0320

26. J. S. Gaffrey, Argone National Laboratory, Environmental Research Division, Bldg. 203, 9700 South Cass Avenue, Argone, IL 60439.

27. P. A. Joyner, Electric Power Research Institute (EPRI), 3412 Hillview Avenue, Palo Alto, CA 94303.

28. S. N. Kondepudi, Electric Power Research Institute (EPRI), 3412 Hillview Avenue, Palo Alto, CA 94303.

29. M. J. Kurylo, NASA, NASA Headquarters, Washington DC 20546-0001.

30. E. R. Kweller, CE-422, 5H-048/FORS, US Department of Energy, 1000 Independence Avenue SW, Washington DC 20585.

31. I. K. Larin, The Institute of Energy Problems of Chemical Physics, Russian Academy of Sciences, Leninsky Prospect, 38, Bldg. 2, 117829 Moscow, Russia.

32. V. G. Khamaganov, The Institute of Energy Problems of Chemical Physics, Russian Academy of Sciences, Leninsky Prospect, 38, Bldg. 2, 117829 Moscow, Russia.

33. C. D. MacCracken, Calmac Manufacturing Corporation, 101 West Sheffield Avenue, Englewood, NJ 07631.

34. M. S. Menzer, Air Conditioning and Refrigeration Institute, 1501 Wilson Blvd., Arlington, VA 22209.

35. M. O. McLinden, National Institute of Standards and Technology, Mail Station 838, Boulder, CO 80303-3328.

36. V. L. Orkin, NIST Chemical Kinetics of Thermodynamics Division, NIST, Gaithersburg, MA 20899.

37-38. OSTI, P. O. Box 62, Oak Ridge, TN 37830. (2 copies)

39. A. R. Ravishankara, United States Department of Commerce, National Oceanic and Atmospheric Administration, 325 Broadway, Boulder, CO 80303-3328.

40. J. B. Shrago, Office of Technology Transfer, 405 Kirkland Hall, Vanderbilt University, Nashville,TN 37240.

41. H. W. Sibley, United Technologies Carrier, P. O. Box 4808, Carrier Parkway, Syacuse, NY 13221.

42. N. D. Smith, Ph.D., Air and Energy Engineering Research Laboratory, U. S. Environmental Protection Agency, Research Triangle Park, NC 27711.

43. G. F. Sowers, P.E., Law Companies Group, Inc., 114 Townpark Drive, Suite 250, Kennesaw, GA 30144-5599.

44. T. G. Statt, Electric Power Research Institute (EPRI), 3412 Hillview Avenue, Palo Alto, CA 94303.

45.   C. M. Walton, Ph.D., Paul D. and Betty Robertson Meek Centennial Professor and Chairman, College of Engineering, University of Texas at Austin, Cockrell Hall, Suite 4.2, Austin, TX 78712.

46.   Office of Assistant Manager for Research and Development, Oak Ridge National Laboratory (ORNL), Oak Ridge, TN 37831-6269.

END

DATE
FILMED
5/3/94